THE INTRINSIC TIME FOR THE SUPG FORMULATION USING QUADRATIC ELEMENTS

Ramon CODINA, Eugenio OÑATE and Miguel CERVERA

Escola Tècnica Superior d'Enginyers de Camins, Canals i Ports
Universitat Politècnica de Catalunya
Jordi Girona Salgado 31, 08034 Barcelona, Spain

Abstract. In this paper the functions of the Péclet number that appear in the intrinsic time of the SUPG formulation are analyzed for quadratic elements. Some related issues such as the computation of the characteristic element length and the introduction of source terms in the one-dimensional model problem are also addressed.

1. Introduction

Besides the interest of the advection-diffusion equation as a mathematical model for several physical phenomena, it represents the starting point for the development of numerical methods for the approximate solution of more complicated transport equations. When the convective terms of these equations become important the standard Galerkin formulation fails and numerical oscillations occur. These oscillations can only be avoided after a drastic refinement of the finite element mesh. The lack of stability that the Galerkin formulation shows in those cases is the common explanation for the nonphysical behaviour of the numerical solution, although an examination of the analytical solution of the discrete equations obtained for the one-dimensional convection-diffusion equation shows the same problem.

The SUPG method (Streamline Upwind/Petrov-Galerkin) introduced by Hughes and Brooks [11],[12] is known to be one of the most efficient procedures for solving convection-dominated equations (for an overview of this method, see [10]).

Our original interest was the development of numerical methods for the solution of the incompressible Navier-Stokes equations using a mixed formulation

in velocities and pressures. It is well known that the interpolation spaces of these two fields must satisfy the so-called Babuška-Brezzi conditions [1],[2] (See also [7]). The simplest elements that verify these conditions are quadratic in velocities (Nevertheless, quadrilateral elements with a bilinear interpolation in velocities and constant pressure have been successfully used in [3] and their possibilities analyzed. See [23]). This, together with the aim of applying the SUPG approach, led us to this work, for which preliminary results have been presented in reference [5].

The original SUPG formulation has undergone several recent improvements that will not be considered here, such as the introduction of discontinuity-capturing terms [6],[15],[19] or the use of the discontinuous Galerkin method in time [18]. The Galerkin/least squares method described in [14] which allows the circumvention of the Babuška-Brezzi conditions [13] will not be considered either. However, all these modifications of the SUPG method share the requirement of a certain parameter, usually called *intrinsic time*, for which proper evaluation greatly influences the accuracy (not the stability) of the numerical solution obtained. Since the very early developments of the SUPG and other Petrov-Galerkin methods for the solution of advection diffusion-equations, the 'optimal' expression for this parameter in terms of the element Péclet number was known for linear elements [9]. Approaches other than the SUPG formulation using quadratic elements have been studied [4],[8]. However, for this one it seems that an 'optimal' intrinsic time for quadratic elements is missing, although using one half of the optimal value for linear elements has been proposed [22]. This choice will be justified in this paper.

An outline of the paper is the following. In section two a short review of the SUPG method is presented. In section three we derive the expressions of the functions that define, in some sense, optimal intrinsic times for one-dimensional quadratic elements. This results in different expressions of these parameters for the different nodes of the element. The possibility of using a unique intrinsic time is then considered. New expressions for the mentioned functions are obtained for hierarchic one-dimensional quadratic elements. This section ends with the proof that optimality is maintained if certain source terms are introduced in the one-dimensional model equation. In section four the extension to multidimensional situations is presented. We propose a methodology for computing the characteristic length of the element and notice the difficulties

inherent to the use of different intrinsic times for the different nodes of the element. In section five several numerical examples are discussed, both for one- dimensional and two-dimensional problems. Finally, some conclusions are drawn.

2. The basis of the SUPG formulation

2.1 The continuous problem

Let Ω be an open bounded domain of $\mathbf{R}^N$ ($N = 1, 2$ or 3) and $\Gamma = \partial\Omega = \overline{\Gamma_D \cup \Gamma_N}$, with $\Gamma_D \cap \Gamma_N = \emptyset$. Consider the convection-diffusion equation

$$\frac{\partial \phi}{\partial t} + \mathbf{u} \cdot \text{ grad } \phi - \text{div}(\mathbf{K} \cdot \text{grad } \phi) = Q \quad , \quad \mathbf{x} \in \Omega \quad , \quad t \in]0, T[, T > 0 \tag{2.1}$$

where $\phi = \phi(\mathbf{x}, t)$ is the unknown function, $\mathbf{u} = \mathbf{u}(\mathbf{x}, t)$ is the velocity field, $\mathbf{K} = \mathbf{K}(\mathbf{x}, t)$ is the diffusion tensor, that we assume is symmetric and positive-definite, and $Q = Q(\mathbf{x}, t)$ is the source term. The boundary and initial conditions for (2.1) are

$$\phi(\mathbf{x}, t) = f(\mathbf{x}, t) \quad , \quad \mathbf{x} \in \Gamma_D \quad , \quad t \in]0, T[\tag{2.2}$$

$$\mathbf{n} \cdot \mathbf{K} \cdot \text{ grad } \phi = h(\mathbf{x}, t) \quad , \quad \mathbf{x} \in \Gamma_N \quad , \quad t \in]0, T[\tag{2.3}$$

$$\phi(\mathbf{x}, 0) = \phi_0(\mathbf{x}) \quad , \quad \mathbf{x} \in \Omega \tag{2.4}$$

In these equations f, h and ϕ_0 are given functions and $\mathbf{n}$ is the unit outward normal to Γ.

Although it is possible to discretize the above problem both in space and time using finite elements [17],[18],[25],[26], we will consider the finite element discretization only in space. This results in an ordinary differential equation in time that can be solved numerically using finite elements or finite differences. For this reason, the variational form of problem (2.1)-(2.4) will be written as follows.

If for a given $t \in]0, T[$ the function $g(\mathbf{x}, t)$ belongs to a space $\mathcal{H}$ of functions defined on Ω, the mapping $t \mapsto g(\cdot, t)$ from $]0, T[$ to $\mathcal{H}$ will also be denoted by $g(t)$. Consider the following function spaces:

$$\mathcal{V} := H^1(\Omega) \tag{2.5}$$

$$\mathcal{V}(g) := \{\varphi \in H^1(\Omega) : \varphi = g \text{ on } \Gamma_D\} \tag{2.6}$$

where g is a given function. The weak form of (2.1)-(2.4), imposing the initial condition in a strong form, is: given $\phi_0 \in L^2(\Omega)$ and $Q :]0,T[\longrightarrow L^2(\Omega)$, find $\phi :]0,T[\longrightarrow \mathcal{V}(f)$ such that

$$\frac{d}{dt}(\phi(t), v) + a(\phi(t), v) = l(v) \quad \forall v \in \mathcal{V}(0) \tag{2.7}$$

$$\phi(0) = \phi_0 \tag{2.8}$$

where $(\cdot,\cdot)$ denotes the inner product of $L^2(\Omega)$, $a(\cdot,\cdot)$ is the bilinear form

$$a(\varphi, v) = \int_\Omega (v\ \mathbf{u} \cdot \mathrm{grad}\varphi + \mathrm{grad}v \cdot \mathbf{K} \cdot \mathrm{grad}\varphi) d\Omega \tag{2.9}$$

and $l(\cdot)$ the linear form

$$l(v) = \int_\Omega v\ Q\ d\Omega + \int_{\Gamma_N} v\ h\ d\Gamma \tag{2.10}$$

2.2 Finite element discretization

Let $\{\Omega^e\}$ be a finite element discretization of the domain Ω, with index e ranging from 1 to the number of elements NE. Consider the spaces:

$$\mathcal{V}^h := \{\varphi \in \mathcal{V} : \varphi|_{\Omega^e} \in P_k(\Omega^e)\} \tag{2.11}$$

$$\mathcal{V}^h(g) := \{\varphi \in \mathcal{V}(g) : \varphi|_{\Omega^e} \in P_k(\Omega^e)\} \tag{2.12}$$

where $P_k(\Omega^e)$ is the set of polynomials of degree at most k on Ω^e. The semidiscrete form of (2.7)-(2.8) using the SUPG method is: find $\phi^h :]0,T[\longrightarrow \mathcal{V}^h(f)$ such that

$$\frac{d}{dt}(\phi^h(t), v)_{su} + a_{su}(\phi^h(t), v) = l_{su}(v) \quad \forall v \in \mathcal{V}^h(0) \tag{2.13}$$

$$\phi^h(0) = \phi_0 \tag{2.14}$$

where

$$(\varphi, v)_{su} = (\varphi, v) + \sum_{e=1}^{NE} \int_{\Omega^e} \tau\ \mathbf{u} \cdot \mathrm{grad}v\ \varphi\ d\Omega \tag{2.15}$$

$$a_{su}(\varphi, v) = a(\varphi, v) + \sum_{e=1}^{NE} \int_{\Omega^e} \tau\ \mathbf{u} \cdot \mathrm{grad}v[\mathbf{u} \cdot \mathrm{grad}\varphi - \mathrm{div}(\mathbf{K} \cdot \mathrm{grad}\varphi)] d\Omega \tag{2.16}$$

$$l_{su}(v) = l(v) + \sum_{e=1}^{NE} \int_{\Omega^e} \tau \ \mathbf{u} \cdot \text{grad}v \ Q \ d\Omega \tag{2.17}$$

The parameter τ in (2.15)-(2.17) is called *intrinsic time*. It will be written as:

$$\tau^e = \frac{\alpha^e \ h^e}{2 \ \|\mathbf{u}^e\|} \tag{2.18}$$

where the e refers to elemental values. Here, $\mathbf{u}^e$ is a characteristic velocity of the element, $\|\mathbf{u}^e\| = (\mathbf{u} \cdot \mathbf{u})^{\frac{1}{2}}$, h^e is a characteristic length and α^e is a nondimensional parameter the expression of which will be discussed in the next section.

REMARKS 2.1

(1) For typical C^0 finite elements, $\tau \ \mathbf{u} \cdot \text{grad}v$ will be discontinuous across interelement boundaries. Since $\mathbf{K} \cdot \text{grad}\phi^h$ will also be discontinuous, the sum of integrals in (2.16) cannot be expressed as a global integral over Ω. The Euler-Lagrange equations for (2.13) are precisely (2.1) and the boundary conditions (2.2) and (2.3) (essential and natural, respectively) together with the additional condition of diffusive-flux continuity across interelement boundaries [12].

(2) For rectangular bilinear elements in 2-D or trilinear elements in 3-D, with $K_{ij} = K \ \delta_{ij}$, K being a positive constant and δ_{ij} the Kronecker delta, we have that $\text{div}(\mathbf{K} \cdot \text{grad}\phi^h) = K\Delta\phi^h \equiv 0$ within each element. This is always the case with linear triangles or tetrahedra. However, this term cannot be neglected if quadratic elements are used.

(3) Equation (2.13) is obtained weighting (2.1) and (2.3) with the function

$$w = v + \tau \ \mathbf{u} \cdot \text{grad}v \tag{2.19}$$

with $\tau \ \mathbf{u} \cdot \text{grad}v$ affecting only the element interiors. Only the diffusive flux multiplied by v can be integrated by parts (using the divergence theorem) □

2.3 Convergence analysis

One of the main attributes of the SUPG formulation for the convection-diffusion equation is that a complete convergence analysis can be performed. This was done in [18] and [21], using the discontinuous Galerkin method in time.

The purpose of this subsection is only to see how the intrinsic time fits in this analysis. For that, we can consider the steady-state problem in (2.1)-(2.3) and the corresponding discrete weak form: find $\phi^h \in \mathcal{V}^h(f)$ such that

$$a_{su}(\phi^h, v) = l_{su}(v) \quad \forall v \in \mathcal{V}^h(0) \tag{2.20}$$

Assuming $K_{ij} = K\ \delta_{ij}$ in (2.1), with $K > 0$, the following error estimate can be proved [18]:

$$|||\phi - \phi^h||| \leq C\ h^{k+\frac{1}{2}}\ \|\phi\|_{k+1} \tag{2.21}$$

where ϕ is the solution of the continuous problem, C is a constant, h is the mesh parameter, $\|\cdot\|_s$ is the norm of the Sobolev space $H^s(\Omega)$, k the degree of the complete polynomial of $\mathcal{V}^h$ and $|||\cdot|||$ is the norm defined by

$$|||w||| := \sqrt{K}\ \|\mathrm{grad} w\|_0 + \sqrt{h}\ \|\mathbf{u}\cdot\mathrm{grad} w\|_0 + \|w\|_0 \tag{2.22}$$

What is important for us is that to prove (2.21), the intrinsic time defined in (2.18) must verify the following conditions:

$$\tau^e \leq C_1\ \frac{(h^e)^2}{K} \quad \text{if} \quad K > h^e\ \|\mathbf{u}^e\| \tag{2.23}$$

$$\tau^e \leq C_2\ \frac{h^e}{\|\mathbf{u}^e\|} \quad \text{if} \quad K < h^e\ \|\mathbf{u}^e\| \tag{2.24}$$

where C_1 and C_2 are constants. Now, let us define the *element Péclet number* as

$$\gamma^e := \frac{\|\mathbf{u}^e\|\ h^e}{2\ K^e} \tag{2.25}$$

where the superscript e in K has been introduced to include the possibility of nonconstant diffusion. From (2.23) and (2.24) it can be seen that if α^e in (2.18) is a function of γ^e (i.e., $\alpha^e = \alpha(\gamma^e)$) then, a *necessary* condition for (2.21) to hold is that

$$\alpha(\gamma^e) = \mathcal{O}(\gamma^e) \quad \text{as} \quad \gamma^e \longrightarrow 0 \tag{2.26}$$

$$\alpha(\gamma^e) = \mathcal{O}(1) \quad \text{as} \quad \gamma^e \longrightarrow \infty \tag{2.27}$$

where $\mathcal{O}$ stands for 'order'. As it will be seen in the following section, the functions α we will obtain satisfy (2.26) and (2.27).

REMARK 2.2

In reference [18] τ^e is set to zero when $K > h^e \ \|\mathbf{u}^e\|$ (diffusion dominated case) $\square$

3. The optimal intrinsic times for one-dimensional quadratic elements

3.1 General considerations

In this section we will consider the one-dimensional steady-state problem (2.1)-(2.4), that in this case reads: find $\phi = \phi(x)$ such that

$$u \frac{d\phi}{dx} - K \frac{d^2\phi}{dx^2} = Q(x), \quad 0 < x < L \tag{3.1}$$

$$\phi(0) = \phi_0, \quad \phi(L) = \phi_L \tag{3.2}$$

where u and K will be considered positive constants, $L > 0$ and ϕ_0 and ϕ_L are given boundary values of the function ϕ. First, we shall assume $Q(x) \equiv 0$ and in subsection 3.6 the introduction of source terms will be addressed.

From here onwards, N will denote a generic shape function of the element and W a weighting function. According to (2.19), this weighting function will be expressed as

$$W(x) = N(x) + \tau \ u \frac{dN}{dx} \tag{3.3}$$

and the intrinsic time of (2.18) as

$$\tau^e = \frac{\alpha^e \ h^e}{2 \ u} \tag{3.4}$$

Throughout this section we assume that $[0, L]$ is discretized using a uniform finite element partition with elements of length h. Thus, the Péclet number $\gamma = uh/2K$ and the parameter α will be the same for all the elements. From (3.3) and (3.4) we have

$$W(x) = N(x) + \frac{\alpha \ h}{2} \frac{dN}{dx} \tag{3.5}$$

where α will depend on the Péclet number γ (see (2.26)-(2.27)). We call the function $\alpha = \alpha(\gamma)$ the *upwind function*. This function will be considered *optimal* if the finite element solution obtained with the weighting functions given by (3.5) is

nodally exact, i.e. both the analytical and the finite element solution of (3.1)-(3.2) take the same values at the nodes of the finite element mesh.

It is well known that for linear elements optimality is attained if $\alpha(\gamma)$ is chosen as

$$\alpha(\gamma) = \coth(\gamma) - \frac{1}{\gamma} \tag{3.6}$$

Our aim is to derive the expressions of the upwind functions using quadratic elements. First, we observe that applying the Galerkin method (i.e, $W = N$) to (3.1)-(3.2) with $Q(x) \equiv 0$ the following difference equations are obtained:

$$[1+\gamma]\phi_{m-1} - [8+4\gamma]\phi_{m-\frac{1}{2}} + 14\phi_m + [-8+4\gamma]\phi_{m+\frac{1}{2}} + [1-\gamma]\phi_{m+1} = 0 \tag{3.7}$$

for the 'extreme' nodes (nodes 1 and 3 in Fig. 1) and

$$[-4-2\gamma]\phi_m + 8\phi_{m+\frac{1}{2}} + [-4+2\gamma]\phi_{m+1} = 0 \tag{3.8}$$

for the 'central' nodes (node 2 in Fig. 1)

******* Insert Fig. 1 *******

The indexes in (3.7) and (3.8) are used according to Fig. 2

******* Insert Fig. 2 *******

Since different equations are obtained for the extreme and the central nodes, it can be anticipated that no single optimal upwind function will exist for quadratic elements. Instead, we will consider

$$W_i(x) = N_i(x) + \frac{\alpha h}{2}\frac{dN_i}{dx} \qquad \text{for } i = 1,3 \tag{3.9}$$

$$W_2(x) = N_2(x) + \frac{\beta h}{2}\frac{dN_2}{dx} \tag{3.10}$$

3.2 The upwind functions α and β

The upwind functions α and β appearing in (3.9) and (3.10) are determined following the same criteria as for linear elements, i.e. by solving analytically the

resulting difference equations obtained applying the SUPG method to (3.1) and (3.2) and by subsequently imposing that the numerical solution be nodally exact.

If the weighting functions (3.9) and (3.10) are used, the new difference equations obtained (instead of (3.7) and (3.8)) are

$$\begin{aligned}&[1-6\alpha+\gamma(1+\alpha)]\phi_{m-1}-[8-12\alpha+\gamma(4+8\alpha)]\phi_{m-\frac{1}{2}}\\&+[14+14\alpha\gamma]\phi_m+[-8-12\alpha+\gamma(4-8\alpha)]\phi_{m+\frac{1}{2}}\\&+[1+6\alpha+\gamma(-1+\alpha)]\phi_{m+1}=0\end{aligned}\tag{3.11}$$

for the extreme nodes and

$$[-4-\gamma(2+4\beta)]\phi_m+[8+8\gamma\beta]\phi_{m+\frac{1}{2}}+[-4+\gamma(2-4\beta)]\phi_{m+1}=0\tag{3.12}$$

for the central nodes. Obtaining $\phi_{m+\frac{1}{2}}$ in terms of ϕ_m and ϕ_{m+1} from (3.12) and the analogous expression of $\phi_{m-\frac{1}{2}}$ in terms of ϕ_{m-1} and ϕ_m and inserting both expressions in (3.11) the following equation is found

$$a_1\phi_{m-1}+a_2\phi_m+a_3\phi_{m+1}=0\tag{3.13}$$

where

$$\begin{aligned}a_1&=3+3\gamma+\gamma^2+3\gamma\beta+\gamma^2\beta+2\gamma^2\alpha+3\gamma^2\alpha\beta\\a_2&=-(6+2\gamma^2+6\gamma\beta+6\gamma^2\alpha\beta)\\a_3&=3-3\gamma+\gamma^2+3\gamma\beta-\gamma^2\beta-2\gamma^2\alpha+3\gamma^2\alpha\beta\end{aligned}\tag{3.14}$$

Since $\lambda=1$ and $\lambda=\frac{a_1}{a_3}$ are the roots of the characteristic polynomial of (3.13) (see [16]), its analytical solution is

$$\phi_m=C_1+C_2\left(\frac{a_1}{a_3}\right)^m\tag{3.15}$$

where C_1 and C_2 are constants depending on the boundary conditions. If x_m is the abcise of the mth nodal point and $\phi(x_m)$ the value of the exact solution of problem (3.1)-(3.2) at this node, it can be readily seen that $\phi_m=\phi(x_m)$ if, and only if

$$\frac{a_1}{a_3}=e^{2\gamma}\tag{3.16}$$

Now, assuming that (3.16) holds, from (3.12) one finds that $\phi(x_{m+\frac{1}{2}})=\phi_{m+\frac{1}{2}}$ if, and only if

$$e^{2\gamma}=\frac{4+\gamma(2+4\beta)+e^{2\gamma}[4-\gamma(2-4\beta)]}{8+8\gamma\beta}\tag{3.17}$$

Assume $\gamma \neq 0$. From (3.17)

$$\beta(\gamma) = \frac{1}{2}\left(\coth\frac{\gamma}{2} - \frac{2}{\gamma}\right) \tag{3.18}$$

and from (3.16)

$$\alpha(\gamma) = \frac{(3+3\gamma\beta)\tanh\gamma - (3\gamma+\gamma^2\beta)}{(2-3\beta\tanh\gamma)\gamma^2} \tag{3.19}$$

The expressions of α and β given by (3.19) and (3.18) are the sought upwind functions. Unfortunately, these expressions look rather more complicated than the corresponding function for linear elements (3.6).

REMARK 3.1

The use of the SUPG formulation with linear elements for homogeneous equations and neglecting the contribution of div($\mathbf{K}$gradϕ) in (2.16) may be interpreted simply as the introduction of numerical diffusion along the streamlines [11]. However, this is not the case for quadratic elements for two reasons: first, the mentioned term div($\mathbf{K}$gradϕ) cannot be neglected, and secondly, the existence of two optimal upwind functions would imply a non-constant added diffusion □

3.3 Asymptotic behaviour of α and β

When linear elements are used, it is common to approximate $\alpha(\gamma)$ given by (3.6) by the function

$$\alpha_a(\gamma) = \begin{cases} \frac{\gamma}{3} & \text{if } 0 \leq \gamma \leq 3 \\ 1 & \text{if } \gamma > 3 \end{cases} \tag{3.20}$$

since $\alpha(\gamma) \to 1$ as $\alpha \to \infty$ and $\alpha(\gamma) = \frac{\gamma}{3} + \mathcal{O}(\gamma^3)$ as $\alpha \to 0$. For the functions $\alpha(\gamma)$ and $\beta(\gamma)$ given by (3.19) and (3.18) a straightforward computation reveals that

$$\begin{aligned} \lim_{\gamma\to\infty} \alpha(\gamma) &= 1 \\ \lim_{\gamma\to\infty} \beta(\gamma) &= \frac{1}{2} \end{aligned} \tag{3.21}$$

Expanding $\alpha(\gamma)$ and $\beta(\gamma)$ in Taylor series in the neighbourhood of $\gamma = 0$, the following expressions are found

$$\begin{aligned} \alpha(\gamma) &= \frac{\gamma}{12} + \mathcal{O}(\gamma^3) \\ \beta(\gamma) &= \frac{\gamma}{12} + \mathcal{O}(\gamma^3) \end{aligned} \tag{3.22}$$

So, (3.19) and (3.18) can be approximated respectively by

$$\alpha_a(\gamma) = \begin{cases} \frac{\gamma}{12} & \text{if } 0 \leq \gamma \leq 12 \\ 1 & \text{if } \gamma > 12 \end{cases} \tag{3.23}$$

$$\beta_a(\gamma) = \begin{cases} \frac{\gamma}{12} & \text{if } 0 \leq \gamma \leq 6 \\ \frac{1}{2} & \text{if } \gamma > 6 \end{cases} \tag{3.24}$$

However, from Figure 3 it is seen that (3.23) and (3.24) do not give such a good approximation to (3.19) and (3.18) respectively as (3.20) does to (3.6). In Figure 3, the upwind functions for linear elements are labelled '*l*'. Functions (3.20), (3.23) and (3.24) are called *asymptotic approximations.*

******* Insert Fig. 3 *******

REMARK 3.2

The upwind functions $\alpha(\gamma)$ and $\beta(\gamma)$ satisfy conditions (2.26) and (2.27) □

3.4 About the possibility of a unique intrinsic time

We have seen that nodally exact results for the solution of (3.1)-(3.2) using the SUPG formulation can only be obtained if the weighting functions (3.9) and (3.10) are used, with α and β given by (3.19) and (3.18). However, one could try to obtain a unique intrinsic time for all the nodes of the element (i.e., $\alpha = \beta$) with another definition of 'optimality'.

An obvious design criterion for the upwind function is that it must not be strongly dependent on the boundary conditions, in the sense that the difference between the values of this function and the functions that give nodally exact results for different boundary conditions should be bounded and as small as possible.

From (3.15) it is seen that if (3.16) holds, the constants C_1 and C_2 that depend on the boundary conditions happen to be the same as the corresponding constants for the analytical solution of (3.1) that are determined from (3.2). Thus, although with a unique upwind function (3.16) will not be satisfied, we can try to obtain this function, say $\alpha^1(\gamma)$, by minimizing the difference

$$a_1 - a_3 e^{2\gamma} \tag{3.25}$$

If in (3.14) we set $\alpha = \beta$ and try to satisfy (3.16), the following equation is obtained

$$P(\alpha) := \alpha^2 + b\alpha + c = 0 \tag{3.26}$$

with

$$b = \frac{1}{\gamma} - \coth(\gamma) \tag{3.27}$$

$$c = \frac{1}{\gamma^2} - \frac{1}{\gamma}\coth(\gamma) + \frac{1}{3} \tag{3.28}$$

The discriminant $\Delta := b^2 - 4c$ of equation (3.26) is plotted in Fig. 4. Since Δ can be negative, (3.26) does not have real roots for all values of γ. However, we could try to minimize $P(\alpha)$, i.e. to choose

$$\alpha_0 = -\frac{1}{2}b = \frac{1}{2}\left(\coth(\gamma) - \frac{1}{\gamma}\right) \tag{3.29}$$

From (3.27)-(3.29) it is easy to see that $b \to -1$, $c \to \frac{1}{3}$ and $\alpha_0 \to \frac{1}{2}$ as $\gamma \to \infty$, and then

$$\lim_{\gamma \to \infty} P(\alpha_0) = \frac{1}{12}$$

So the function

$$\alpha^1(\gamma) = \frac{1}{2}\left(\coth(\gamma) - \frac{1}{\gamma}\right) \tag{3.30}$$

seems to be a good candidate for use as the upwind function since, although (3.26) is not fulfilled, $P(\alpha^1)$ remains small. In Fig. 4 this value is represented against the Péclet number.

******* Insert Fig. 4 *******

Like the function $\alpha^l(\gamma)$ given by (3.6), $\alpha^1(\gamma)$ can be approximated by

$$\alpha_a^1(\gamma) = \begin{cases} \frac{\gamma}{6} & \text{if } 0 \le \gamma \le 3 \\ \frac{1}{2} & \text{if } \gamma > 3 \end{cases} \tag{3.31}$$

The function $\alpha^1(\gamma)$ given by (3.30) is represented in Fig. 5, together with $\alpha(\gamma)$ and $\beta(\gamma)$ of (3.19) and (3.18), for purposes of comparison.

***** Insert Fig. 5 *****

REMARK 3.3

The function $\alpha^1(\gamma)$ given by (3.30) has been proposed in [22] as the result of numerical experiments □

3.5 The functions α and β for hierarchic elements

The objective of this section is to investigate how sensitive the optimal upwind functions are to the interpolation used within each element. This sensitivity is a clear handicap when the previous concepts have to be applied in multidimensional situations, in which case the expressions of the shape functions take different forms depending on the direction one considers. This will be discussed in more detail in section four.

Now, let us consider the unknown function $\phi(x)$ interpolated within each element as

$$\phi(x) \approx N_1(x)\phi_1 + N_2(x)\Delta\phi_2 + N_3(x)\phi_3 \tag{3.32}$$

where N_1, N_2 and N_3 are the shape functions shown in Fig. 6, ϕ_1, ϕ_2 and ϕ_3 the nodal values of ϕ and $\Delta\phi_2$ the difference between ϕ_2 and the linear interpolation at node 2 obtained from ϕ_1 and ϕ_3.

***** Insert Fig. 6 *****

A similar analysis to that made in subsection 3.2 shows that the optimal upwind functions are now given by

$$\beta^h(\gamma) = \frac{1}{2} + \frac{1}{e^\gamma - 1} - \frac{1}{\gamma} \tag{3.33}$$

$$\alpha^h(\gamma) = \left(1 + \frac{1}{\gamma\beta}\right)\coth(\gamma) - \left(\frac{1}{3\beta} + \frac{1}{\gamma^2\beta} + \frac{1}{\gamma}\right) \tag{3.34}$$

where the label 'h' refers to the hierarchic formulation of the element. The asymptotic behaviour of the upwind function α^h is completely different to the corresponding α given by (3.19), whereas the asympotic behaviour of β^h is similar to that of the function β in (3.18). In fact, now we have that $\beta^h \to \frac{1}{2}$, $\alpha^h \to \frac{1}{3}$ as

$\gamma \to \infty$ and

$$\alpha^h(\gamma) = \frac{1}{15}\gamma + \mathcal{O}(\gamma^2)$$

$$\beta^h(\gamma) = \frac{1}{12}\gamma + \mathcal{O}(\gamma^2)$$

in the neighbourhood of $\gamma = 0$. So, the asymptotic approximations for α^h and β^h will be

$$\alpha_a^h(\gamma) = \begin{cases} \frac{\gamma}{15} & \text{if } 0 \le \gamma \le 5 \\ \frac{1}{3} & \text{if } \gamma > 5 \end{cases} \tag{3.35}$$

$$\beta_a^h(\gamma) = \begin{cases} \frac{\gamma}{12} & \text{if } 0 \le \gamma \le 6 \\ \frac{1}{2} & \text{if } \gamma > 6 \end{cases} \tag{3.36}$$

We see that $\beta_a^h(\gamma) = \beta_a(\gamma)$ (see (3.23)) but $\alpha_a^h(\gamma)$ and $\alpha_a(\gamma)$ differ totally (see (3.23)).

In Figure 7 the functions $\alpha^h(\gamma)$ of (3.34) and $\beta^h(\gamma)$ of (3.33) are represented.

******* Insert Fig. 7 *******

The main conclusion of this analysis is that special care must be taken in the finite element interpolation . Even if only an approximation of the upwind function is required, accuracy is highly influenced by this approximation. Too diffusive results are obtained if the upwind function is overestimated, whereas oscillations may occur if it is underestimated.

3.6 Introduction of source terms

Up to now, we have only considered the homogeneous equation (3.1), i.e., with $Q(x) \equiv 0$. We have proved that the upwind functions (3.18) and (3.19) give nodally exact solutions in this case. Now we can prove that in fact this is also true for certain functions $Q(x)$.

In order to place the problem within a general framework, let us assume that the continuous problem can be written as

$(A.C)$ Find $\phi \in \mathcal{V}(f)$ such that $a(\phi, v) = l(v) \quad \forall v \in \mathcal{V}(0)$

For the sake of clarity, we will consider that the function spaces $\mathcal{V}$ and $\mathcal{V}(f)$ are those given by (2.5) and (2.6). This problem is defined by a bilinear form $a(\cdot,\cdot)$ and a linear form $l(\cdot)$. We also need to consider the problems

$(B.C)$ Find $\phi \in \mathcal{V}(0)$ such that $a(\phi, v) = l(v) \quad \forall v \in \mathcal{V}(0)$

$(C.C)$ Find $\phi \in \mathcal{V}(f)$ such that $a(\phi, v) = 0 \quad \forall v \in \mathcal{V}(0)$

The discrete problems corresponding to (A.C), (B.C) and (C.C) will be denoted (A.D), (B.D) and (C.D) respectively. These problems are obtained simply by replacing $\mathcal{V}$, $\mathcal{V}(f)$ and $\mathcal{V}(0)$ by $\mathcal{V}^h \subset \mathcal{V}$, $\mathcal{V}^h(f) \subset \mathcal{V}(f)$ and $\mathcal{V}^h(0) \subset \mathcal{V}(0)$. The spaces $\mathcal{V}^h$ and $\mathcal{V}^h(f)$ are those defined in (2.11) and (2.12). We assume that all these problems have a unique solution.

Now, let $\pi : \mathcal{V} \longrightarrow \mathcal{V}^h$ be the projection from $\mathcal{V}$ to $\mathcal{V}^h$ defined by $\pi(\varphi) = \tilde{\varphi}$, the finite element interpolant of φ. In this context, a solution ϕ of (A.D) can be defined to be nodally exact if the solution ϕ^* of (A.C) verifies $\pi(\phi^*) = \phi$.

REMARK 3.4

The bilinear form $a(\cdot,\cdot)$ and the linear form $l(\cdot)$ can arise from any *consistent* weighted residual method, for example the SUPG □

The result we wish to prove is

Proposition. *If there exists a function $\psi \in \mathcal{V}^h$ such that*

$$a(\psi, v) = l(v) \quad \forall v \in \mathcal{V}(0) \tag{3.37}$$

then, if problem (C.D) has a nodally exact solution, so does (A.D).

Proof. We first observe that if (C.D) has a nodally exact solution (n.e.s.), then such a solution can be obtained for (A.D) if, and only if, it can be obtained for (B.D). To see this, let ϕ be a n.e.s. for (A.D) and ϕ_1 a n.e.s. for (C.D). Put $\phi_2 = \phi - \phi_1$. Then $\phi_2 \in \mathcal{V}^h(0)$ and $a(\phi_2, v) = a(\phi, v) - a(\phi_1, v) = l(v) \ \ \forall v \in \mathcal{V}^h(0)$, so ϕ_2 is a n.e.s. for (B.D), since π is linear. Reciprocally, let ϕ_2 and ϕ_1 be n.e.s. for (B.D) and (C.D) respectively. Then $\phi = \phi_1 + \phi_2 \in \mathcal{V}^h(f)$ and $a(\phi, v) = a(\phi_1, v) + a(\phi_2, v) = l(v) \ \ \forall v \in \mathcal{V}^h(0)$. ϕ will be a n.e.s. for (A.D).

Now we prove that a n.e.s. for (B.D) can be obtained. By (3.37) this problem can be stated as: find $\phi \in \mathcal{V}^h(0)$ such that $a(\phi, v) = a(\psi, v) \ \ \forall v \in \mathcal{V}^h(0)$, since

$\mathcal{V}^h(0) \subset \mathcal{V}(0)$. Set $\delta = \phi - \psi$. δ is the solution of: find $\delta \in \mathcal{V}^h(-\psi)$ such that $a(\delta, v) = 0 \quad \forall v \in \mathcal{V}^h(0)$. This problem has the form (C.D), so δ can be computed nodally exact. Let δ^* and ϕ^* be the solutions of the continuous problems (C.C) and (B.C) corresponding to the discrete problems for δ and ϕ. Since $\psi \in \mathcal{V}^h$, and using again (3.37), $\delta^* = \phi^* - \psi$, and so

$$\begin{aligned}\pi(\phi^*) &= \pi(\delta^* + \psi) \\ &= \pi(\delta^*) + \pi(\psi) \quad (\pi \text{ is linear}) \\ &= \delta + \psi = \phi \quad (\delta \text{ is a n.e.s and } \psi \in \mathcal{V}^h)\end{aligned}$$

Since $\pi(\phi^*) = \phi$, we have that ϕ is a n.e.s. for (B.D) □

REMARKS 3.5

(1) In our case, the forms $a(\cdot,\cdot)$ and $l(\cdot)$ will not be given by (2.9) and (2.10) but by (2.16) and (2.17). This does not introduce any trouble since the solution of problem (2.1)-(2.4) satisfies (2.13)-(2.14).

(2) Easily speaking, condition (3.37) means that the equation of the continuous problem has a solution, not necessarily satisfying the boundary conditions, that belongs to the space of interpolation functions. Thus, although we know how to obtain nodally exact solutions for (3.1)-(3.2) only with $Q(x) \equiv 0$ using quadratic elements, the same procedure will give nodally exact solutions for source terms elementwise linear, since if $Q(x) = ax+b$, with a and b constants, the general solution of (3.1) is, for $u \neq 0$:

$$\phi(x) = C_1 + C_2 e^{\frac{u}{K}x} + \frac{a}{2u}x^2 + \left(\frac{b}{u} + \frac{aK}{u^2}\right)x \tag{3.38}$$

where C_1 and C_2 are constants to be determined from the boundary conditions. Setting $C_2 = 0$ we obtain a function that belongs to the interpolation space, i.e., satisfies (3.37) □

4. Multidimensional convection-diffusion equation

In order to compute the intrinsic time given by (2.18) for each element in the multidimensional convection-diffusion equation (2.1), the values of h^e, K^e and $\mathbf{u}^e$ that give the Péclet number (2.25) are needed. We must also know which is the expression of the upwind function $\alpha^e = \alpha(\gamma^e)$ that corresponds to the node under consideration.

We compute the velocity $\mathbf{u}^e$ simply as the average of the nodal velocities of the element and K^e as the diffusion along the flow direction. Since we have assumed that $\mathbf{K}$ in (2.19) is a second order tensor, this diffusion will be

$$K^e = \frac{u_i{}^e K_{ij} u_j{}^e}{\|\mathbf{u}^e\|^2} \tag{4.1}$$

where the sum convention is used.

The computation of h^e and the choice of the upwind function will be explained in more detail.

4.1 The characteristic length

To simplify the notation we will consider the two-dimensional case, although what follows is completely general.

Let $\mathcal{D}$ be a convex domain in $\mathbf{R}^2$ transformed into $\mathcal{D}' \subset \mathbf{R}^2$ by an affine mapping $\mathbf{f} = (f_1, f_2)$.

******* Insert Fig. 8 *******

Using the notation of Fig. 8, let

$$l = \|B - A\| \quad , \quad l' = \|B' - A'\| \tag{4.2}$$

and $\mathbf{v}' = (\mathbf{Df})\mathbf{v}$, where $\mathbf{Df}$ is the Jacobian matrix of $\mathbf{f}$. Since

$$\begin{aligned} \mathbf{f}(B) &= \mathbf{f}(A) + l' \frac{\mathbf{v}'}{\|\mathbf{v}'\|} \\ &= \mathbf{f}(A) + (\mathbf{Df})(B - A) \end{aligned} \tag{4.3}$$

we have that

$$l' \frac{\mathbf{v}'}{\|\mathbf{v}'\|} = (\mathbf{Df})(B - A),$$

$$\begin{aligned} l'(\mathbf{Df})^{-1}\mathbf{v}' &= l'\mathbf{v} \\ &= \|\mathbf{v}'\|(B - A) \end{aligned} \tag{4.4}$$

and taking the Euclidian norm on both sides of (4.4)

$$l' = \frac{\|\mathbf{v}'\|}{\|\mathbf{v}\|} l \tag{4.5}$$

Formula (4.5) allows to compute the characteristic length in the flow direction as

$$h^e = \frac{\|\mathbf{u}^e\|}{\|\mathbf{u}^e{}_N\|} h_N \tag{4.6}$$

where index N indicates that the value corresponds to the parent domain of the element with 'natural' coordinates (ξ, η). Equation (4.6) reduces the computation of h^e to that of h_N, which can be easily estimated since the geometry is now very simple. In our computations we have taken, for the parent domains of Fig. 9:

$h_N = 2$ for quadrilateral elements

$h_N = 0.7$ for triangular elements

******* Insert Fig. 9 *******

REMARKS 4.1

(1) The length h^e defined by (4.6) depends on the point (x, y) of Ω^e. Thus, it will be numerically different at each integration point. Also, the exact value of h_N depends on each point, although the assumption of a constant value seems reasonable.

(2) From (4.3) it can be seen that (4.6) will be exact whenever the mapping $\mathbf{f}$ can be considered affine. This will always be the case with straightsided triangles and parallelograms in two dimensions.

(3) In references [15] and [20], formula (4.6) with $h_N = 2$ was suggested heuristically, without defining its limits of validity. Note that the parametrization of the parent domain defines h_N □

4.2 Assignment of upwind functions

In section 3, the expressions of the upwind functions α and β for quadratic elements were obtained. The weighting function of a certain node of an element will be obtained using α or β depending on the position of the node. Clearly, in multidimensional situations this position is relative to the direction of the flow, which complicates the definition of a node as 'extreme' or 'central'. This, of course, is an important drawback for the use of different upwind functions.

The heuristic criterion we have followed is based on the assignment of upwind functions taking into account whether a node is extreme or central for certain

directions of the flow. For 2-D elements, we have taken these directions as those defined by the coordinates ξ, η (see Fig. 10) for the nine-noded Lagrangian element and those defined by the area coordinates $1-\xi-\eta$, ξ and η for the six-noded triangle. For the corner nodes of the elements the function α has been chosen and for the interior node of the nine-noded element the function β. The problem arises when the upwind function for the midside nodes must be determined. For example, the shape function of node 5 for the nine-noded element (see Fig. 10) along the $\eta = -1$ line corresponds to the shape functions of node 2 in Figure 1, i.e. a central node, whereas along the $\xi = 0$ line the corresponding shape function is that of node 1 in Fig. 1, an extreme node. So, the upwind function of node 5, say δ_5, will be taken as a combination of functions α and β. In Figure 10, the nodal numbering in the parent domain and the chosen upwind functions are indicated.

******* Insert Fig. 10 *******

The best numerical results have been obtained taking δ_i as the functions

$$\delta_i = f_i(\theta)\alpha + [1 - f_i(\theta)]\beta \tag{4.7}$$

where for the six-noded element

$$\begin{aligned} f_4(\theta) &= \sin^2\theta \\ f_5(\theta) &= f_4(\theta - \frac{\pi}{4}) \\ f_6(\theta) &= \cos^2\theta \end{aligned} \tag{4.8}$$

and for the nine noded element

$$\begin{aligned} f_5(\theta) = f_7(\theta) &= \sin^2\theta \\ f_6(\theta) = f_8(\theta) &= \cos^2\theta \end{aligned} \tag{4.9}$$

In (4.7)-(4.9), θ is the angle shown in Figure 10.

REMARK 4.2

Notice that for bilinear quadrilateral elements the expression of the upwind function will not be the 'optimal' if the velocity is not parallel to the edges, since the shape functions are not linear along those directions □

5. Numerical examples

The examples presented in this section have been run on a CONVEX-C120 computer using double precision.

5.1 One-dimensional problems

EXAMPLE 1. In this example we solve problem (3.1)-(3.2) with $u = 1$, $K = 0.01$, $Q(x) = \sin(\pi x)$, $L = 1$ and $\phi_0 = \phi_L = 0$. The interval $[0, 1]$ is discretized using ten quadratic elements of equal length 0.1. This gives the value $\gamma = 5$ for the Péclet number. The analytical solution is

$$\phi(x) = C_1 + C_2 e^{\frac{u}{K}x} + \frac{K}{u^2 + K^2\pi^2}\left[\sin(\pi x) - \frac{u}{K\pi}\cos(\pi x)\right] \tag{4.10}$$

with

$$C_2 = \frac{2u}{(u^2\pi + K^2\pi^3)(1 - e^{-\frac{u}{K}})} \tag{4.11}$$

$$C_1 = -\frac{1}{2}(1 + e^{\frac{u}{K}})C_2 \tag{4.12}$$

Condition (3.37) is not fulfilled and in fact nodally exact solutions are not obtained. However, the use of the optimal upwind functions of (3.18) and (3.19) gives results (Figure 11.*a*) that cannot be distinguished from those of the analytical solution (linear interpolation between nodes has been used in the plots). In Figure 11.*b* the solution obtained using the unique function (3.30) is plotted and Fig. 12 shows the relative error (in percentage) obtained using the two methods.

******* Insert Fig. 11 *******

******* Insert Fig. 12 *******

We observe that the use of (3.30) gives a solution that smooths the right boundary layer.

EXAMPLE 2. In this case we solve the transient problem

$$\frac{\partial\phi}{\partial t} + u\frac{\partial\phi}{\partial x} - K\frac{\partial^2\phi}{\partial x^2} = 0, \quad 0 < x < 1, \quad t > 0 \tag{4.13}$$

$$\phi(0,t) = 0, \quad t > 0 \tag{4.14}$$

$$\phi(1,t) = 1, \quad t > 0 \tag{4.15}$$

$$\phi(x,0) = x, \quad 0 < x < 1 \tag{4.16}$$

The analytical solution for this problem can be expressed as

$$\phi(x,t) = x + \sum_{n=1}^{\infty} \frac{B_n}{A_n} \left(1 - e^{-A_n t}\right) e^{\frac{u}{2K}x} \sin(n\pi x) \tag{4.17}$$

with

$$A_n = \frac{u^2}{2K} + K(n\pi)^2 \tag{4.18}$$

$$B_n = \frac{2nu\pi}{\frac{u^2}{4K^2} + n^2\pi^2} \left[(-1)^n e^{-\frac{u}{2K}} - 1\right] \tag{4.19}$$

We have taken $u = 1$ and $K = 0.02$. Again, ten quadratic elements of length 0.1 have been used. The ordinary differential equation that results after space discretization has been solved using the Crank-Nicolson scheme. Based on the results in reference [24], the time step has been taken as $\Delta t = 0.05$, which gives a Courant number $C := \frac{2u\Delta t}{h} = 1$. In Fig. 13 the solution obtained applying the Galerkin procedure is shown for $t = 0, 0.25, 0.5, 1$ and 2 (using a linear interpolation between nodal values for plotting). Observe that for this rather small Péclet number (γ=2.5) oscillations occur even at an early stage.

******* Insert Fig. 13 *******

In Figures 14.*a* and 14.*b* the solution obtained with the optimal upwind functions (3.18) and (3.19) and the upwind function (3.30) are represented. The first result is undistinguishable from the analytical solution (4.17)-(4.19). Again, the smoothing of the right boundary layer when using (3.30) can be observed.

******* Insert Fig. 14 *******

EXAMPLE 3. We consider in this example the Burgers' equation

$$\frac{\partial u}{\partial t} + u\frac{\partial u}{\partial x} - \nu\frac{\partial^2 u}{\partial x^2} = 0, \quad 0 < x < 1, \quad t > 0 \tag{4.20}$$

with boundary and initial conditions

$$u(0,t) = 0, \quad t > 0 \tag{4.21}$$

$$u(1,t) = 1, \quad t > 0 \tag{4.22}$$

$$u(x,0) = x, \quad 0 < x < 1 \tag{4.23}$$

The nonlinear equation (4.20) has been solved using the secant Newton method. In this case, a convection-diffusionlike equation must be solved for each iteration. The interval $[0, L]$ has been discretized using ten equal-length quadratic elements. The Crank-Nicolson scheme with $\Delta t = 0.05$ has been used in time. The viscosity ν has been taken as $\nu = 10^{-4}$, which gives an element Reynolds number $Re := \frac{uh}{2\nu} = 2500$. The convergence criterion has been chosen as $\|u_n^i - u_n^{i-1}\|_\infty < 10^{-8}$, where u_n^j is the value of u at the jth iteration of the nth time step. Four iterations were needed for the SUPG formulation and six for the Galerkin method.

The qualitative shape of the solution $u(x,t)$ of (4.20)-(4.23) may be predicted if we take $\nu = 0$ in (4.20) and solve this equation with the conditions (4.21) and (4.23). In this case, the analytical solution is

$$u(x,t) = \frac{x}{1+t} \tag{4.24}$$

i.e., a straightline with slope decreasing in time.

In Figure 15, the Galerkin solution for $t = 1$ is shown. As expected, high oscillations occur.

******* Insert Fig. 15 *******

The solutions with the SUPG formulation are depicted in Figures 16.*a* and 16.*b*, using the upwind functions of (3.18) and (3.19) and that given by (3.30), respectively. A better resolution of the right boundary layer is obtained in the first case.

******* Insert Fig. 16 *******

5.2 Two-dimensional problems

EXAMPLE 4. The steady-state case in equation (2.1) with the boundary conditions (2.2) and (2.3) has been solved, with:

$$\Omega = \left]\frac{-1}{2},\frac{1}{2}\right[\times \left]\frac{-1}{2},\frac{1}{2}\right[$$
$$\Gamma_D = \partial\Omega, \quad \Gamma_N = \emptyset$$
$$\mathbf{u}(x,y) = \left(\frac{\sqrt{2}}{2},\frac{\sqrt{2}}{2}\right)$$
$$K_{ij}(x,y) = 2\cdot 10^{-2}\delta_{ij}$$
$$Q(x,y) = 5$$
$$f(x,y) = 0$$

The domain Ω has been discretized using a uniform finite element mesh with 21×21 nodes in all the cases. The resulting Péclet number is $\gamma = 2.5$ for quadratic elements ($h \approx 0.1$) and $\gamma = 1.25$ for linear elements ($h \approx 0.05$). This example was chosen for testing the adopted expressions (4.7)-(4.9). Results obtained with quadratic and linear quadrilaterals and triangular elements and using the optimal upwind functions of (3.18) and (3.19) are shown in Fig. 17. The results obtained for quadratic elements are almost the same as for linear elements.

******* Insert Fig. 17 *******

EXAMPLE 5. This and the following examples have been taken from reference [15]. Now, equation (2.1) with $\frac{\partial\phi}{\partial t} \equiv 0$ and the boundary conditions (2.2) and (2.3) is solved, with:

$$\Omega = \left]\frac{-1}{2},\frac{1}{2}\right[\times \left]\frac{-1}{2},\frac{1}{2}\right[- \{0\} \times \left]\frac{-1}{2},0\right]$$
$$\Gamma_D = \partial\Omega, \quad \Gamma_N = \emptyset$$
$$\mathbf{u}(x,y) = (-y,x)$$
$$K_{ij}(x,y) = 10^{-8}\delta_{ij}$$
$$Q(x,y) = 0$$
$$f(x,y) = \begin{cases} \sin\pi(1+2y) & \text{if } x = 0 \text{ and } -\frac{1}{2} \le y \le 0 \\ 0 & \text{else} \end{cases}$$

In all the cases, 31×31 nodal points and a uniform finite element mesh have been used. For the small diffusion considered, the solution of this problem is

just the advection of the sine profile. The objective of this problem was only to test the accuracy of the algorithm, since the exact solution is very smooth and the Galerkin method only produces small amplitude oscillations. Results obtained with different quadrilateral and triangular elements using the optimal upwind functions are depicted in Figure 18. Similar accuracy is obtained in all the cases.

******* Insert Fig. 18 *******

EXAMPLE 6. Again, the steady-state problem (2.1)-(2.3) is solved, now with:

$$\Omega = \left]\frac{-1}{2},\frac{1}{2}\right[\times \left]\frac{-1}{2},\frac{1}{2}\right[$$
$$\Gamma_D = \partial\Omega, \quad \Gamma_N = \emptyset$$
$$\mathbf{u}(x,y) = (\cos\theta, -\sin\theta)$$
$$K_{ij}(x,y) = 10^{-6}\delta_{ij}$$
$$Q(x,y) = 0$$
$$f(x,y) = \begin{cases} 1 & \text{if } (x,y) \in \Gamma_{D1} \\ 0 & \text{if } (x,y) \in \Gamma_{D2} \end{cases}$$

with

$$\Gamma_{D1} = \left\{-\frac{1}{2}\right\} \times \left[\frac{1}{4},\frac{1}{2}\right] \cup \left]-\frac{1}{2},\frac{1}{2}\right[\times \left\{\frac{1}{2}\right\}$$

$$\Gamma_{D2} = \Gamma_D - \Gamma_{D1}$$

This problem shows the inability of the SUPG formulation to preclude overshoots and undershoots when sharp layers are present.

We have solved this problem with the angles θ given by $\tan\theta = \frac{1}{2}$, 1 and 2. The results shown in Figs. 19, 20 and 21 correspond to the latter case, when overshoots and undershoots are more important. However, it is seen that they are bigger using linear elements than using quadratic elements. The solution obtained using the upwind functions (3.18) and (3.19) together with (4.7)-(4.9) looks better than that obtained with the single upwind function (3.30), although the different computational effort must be also considered.

******* Insert Fig. 19 *******

***** Insert Fig. 20 *****

***** Insert Fig. 21 *****

6. Conclusions

In this paper we have derived the expressions of the upwind functions that give nodally exact results for the one-dimensional steady-state convection-diffusion equation using the SUPG formulation with quadratic elements. In this case, two different functions are needed, one for the 'extreme' nodes and another one for the 'central' node. This complicates the extension to multidimensional problems, although good results have been obtained with the methodology proposed in the paper. Also, the possibility of a unique upwind function has been studied. The obtained results are not so good, but the greater simplicity of this procedure must also be considered for practical purposes. In fact, in that case there is no more computational work due to the SUPG method needed than for linear elements. On the other hand, the feasibility of using different intrinsic times in the case of elements of order higher than two seems very restricted.

Acknowledgements

The authors wish to thank Knut Eckstein for his help in preparing some of the numerical results. The first author also acknowledges the economic support of the CIRIT (Generalitat de Catalunya).

References

[1] I. Babuška. Errors bounds for finite element method. *Numer. Math.*, vol. 16 (1971) 322–333.

[2] F. Brezzi. On the existence, uniqueness and approximation of saddle point problems arising from Lagrange multipliers. RAIRO, *Ser. Rouge Anal. Num.*, vol. 8, R-2 (1976).

[3] A.N. Brooks and T.J.R. Hughes. Streamline Upwind/Petrov-Galerkin formulations for convective dominated flows with particular emphasis on the

incompressible Navier-Stokes equations. *Comp. Meth. in Appl. Mech. and Engng.*, vol. 32, (1982) 199–259.

[4] I. Christie and A.R. Mitchell. Upwinding of high order Galerkin methods in conduction-convection problems. *Int. J. Num. Met. in Engng.*, vol. 14 (1978) 1764–1771.

[5] R. Codina, E. Oñate, M. Cervera and K. Eckstein. Una formulación de Petrov-Galerkin para el análisis de problemas de convección-difusión con elementos finitos cuadráticos. *Proc. of the First Conference on Numerical Methods in Engineering, SEMNI*, Gran Canaria, Spain, 1990.

[6] A.C. Galeão and E.G. Dutra do Carmo. A consistent approximate upwind Petrov-Galerkin method for convection-dominated problems. *Comp. Meth. in Appl. Mech. and Engng.*, vol. 68 (1988) 83–95.

[7] V. Girault and P.A. Raviart. *Finite element methods for Navier-Stokes equations* (Springer-Verlag, 1986).

[8] J.C. Heinrich. On quadratic elements in finite element solutions of steady-state convection-diffusion equations. *Int. J. Num. Met. in Engng.* vol. 15 (1980) 1041–1052.

[9] J.C. Heinrich and O.C. Zienkiewicz. The finite element method and 'upwinding' techniques in the numerical solution of convection dominated flow problems, in: *Finite Element Methods for Convection Dominated Flows*, T.J.R. Hughes (ed.) (1979).

[10] T.J.R. Hughes. Recent progress in the development and understanding of SUPG methods with special reference to the compressible Euler and Navier-Stokes equations, in: *Finite elements in fluids*, vol. 7, R.H. Gallagher; R. Glowinski, P.M. Gresho, J.T. Oden and O.C. Zienkiewicz (eds.) (1987).

[11] T.J.R. Hughes and A. Brooks. A multi-dimensional upwind scheme with no crosswind diffusion, in: *FEM for convection dominated flows*, T.J.R. Hughes (ed.) ASME, New York (1979).

[12] T.J.R. Hughes and A.N. Brooks. A theoretical framework for Petrov-Galerkin methods, with discontinuous weighting functions: applications to the streamline upwind procedure, in: *Finite Element in fluids*, R.H. Gallagher, D.M. Norrie, J.T. Oden and O.C. Zienkiewicz (eds.), vol. IV, (Wiley, London, 1982) 46–65.

[13] T.J.R. Hughes, L.P. Franca and M. Balestra. A new finite element formulation for computational fluid dynamics: V. Circumventing the Babuška-Brezzi condition: a stable Petrov- Galerkin formulation for the Stokes problem accommodating equal- order interpolations. *Comp. Meth. in Appl. Mech. and Engng.*, vol. 59 (1986) 85–99.

[14] T.J.R. Hughes, L.P. Franca and G.M. Hulbert. A new finite element formulation for computational fluid dynamics: VIII. The Galerkin/least-squares method for advective-diffusive equations. *Comp. Meth. in Appl. Mech. and Engng.*, vol. 73 (1989) 173–189.

[15] T.J.R. Hughes, M. Mallet and A. Mizukami. A new finite element formulation for computational fluid dynamics: II. Beyond SUPG. *Comp. Meth. in Appl. Mech. and Engng.*, vol. 54 (1986) 341–355.

[16] Isaacson, E. and H.E. Keller. *Analysis of numerical methods.* (John Wiley & Sons, 1966)

[17] C. Johnson. The Streamline Diffusion finite element method for compressible and incompressible fluid flow. *Von Karman Lecture Series, IV: Computational Fluid Dynamics* (March 1990)

[18] C. Johnson, U. Nävert and J. Pitkaranta. Finite element methods for linear hyperbolic equations *Comp. Meth. in Appl. Mech. and Engng.*, vol. 45 (1984) 285–312.

[19] C. Johnson, A. Szepessy and P. Hansbo. On the convergence of shock-capturing streamline-diffusion finite element methods for hyperbolic conservation laws. To appear in *Math. Comp.*

[20] M. Mallet. *A finite element method for computational fluid dynamics.* Ph.D. Thesis. Stanford University (1985)

[21] U. Nävert. *A finite element method for convection-diffusion problems.* Ph.D. Thesis. Chalmers University of Technology, Göteborg, Sweden (1982)

[22] F. Shakib. *Finite element analysis of the compressible Euler and Navier-Stokes equations.* Ph.D. Thesis. Stanford University (1988).

[23] P. Le Tallec and V. Ruas. On the convergence of the bilinear-velocity constant-pressure finite element method in viscous flow. *Comp. Meth. in Appl. Mech. and Engng.*, vol. 54 (1986) 235–243.

[24] T.E. Tezduyar and D.K. Ganjoo. Petrov-Galerkin formulations with

weighting functions dependent upon spatial and temporal discretization: application to transient convection-diffusion problems. *Comp. Meth. in Appl. Mech. and Engng.*, vol. 59 (1986) 49–71.

[25] C.C. Yu and J.C. Heinrich. Petrov-Galerkin methods for the time-dependent convective transport equation. *Int. J. Num. Met. in Engng.*, vol. 23 (1986) 883–901.

[26] C.C. Yu and J.C. Heinrich. Petrov-Galerkin methods for multidimensional time-dependent convective transport equation. *Int. J. Num. Met. in Engng.*, vol. 24 (1987) 2201–2215.

LIST OF FIGURES

- Fig. 12. Relative errors for the solutions *a* and *b* of Fig. 11

- Fig. 13. Galerkin solution of example 2

- Fig. 14. Solutions of example 2. *a*) Using the upwind functions (3.18) and (3.19). *b*) Using the unique upwind function (3.30)

- Fig. 15. Galerkin solution of example 3

- Fig. 16. Solutions of example 3. *a*) Using the upwind functions (3.18) and (3.19). *b*) Using the unique upwind function (3.30)

- Fig. 17. Results of example 4 using elements of 3, 4, 6 and 9 nodes

- Fig. 18. Results of example 5 using elements of 3, 4, 6 and 9 nodes

- Fig. 19. Results of example 6 using 3-noded linear triangular and 4-noded bilinear quadrilateral elements

- Fig. 20. Results of example 6 using quadratic triangular (6 nodes) and biquadratic quadrilateral (9 nodes) elements with the upwind functions (3.18) and (3.19)

- Fig. 21. Results of example 6 using quadratic triangular (6 nodes) and biquadratic quadrilateral (9 nodes) elements with the upwind function (3.30)

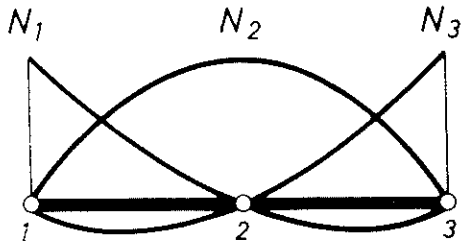

Fig. 1. Three noded quadratic element and shape functions

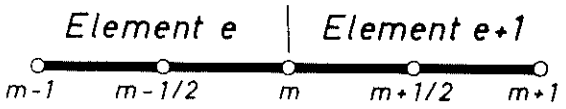

Fig. 2. Indexes referring the nodes of two adjacent elements

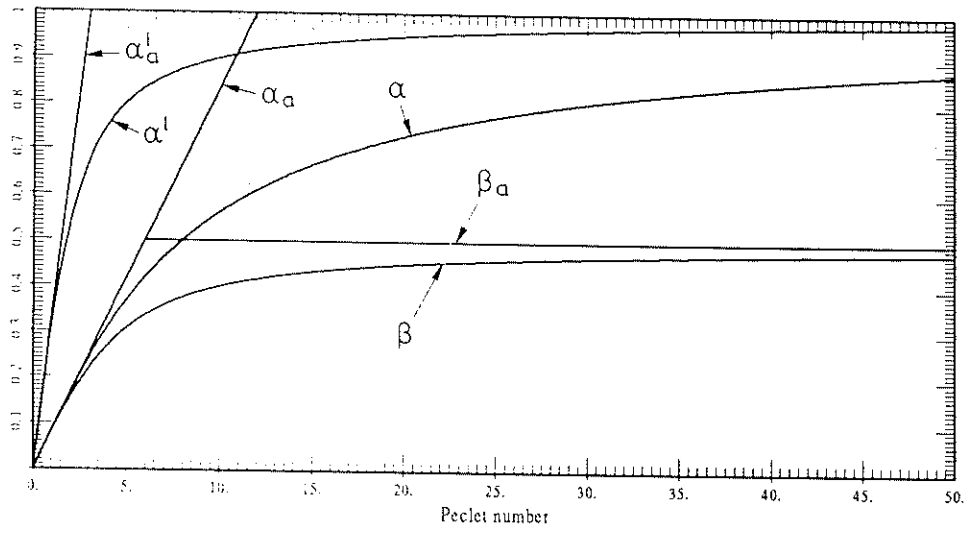

Fig. 3. Upwind functions for linear and quadratic elements and their asymptotic approximations

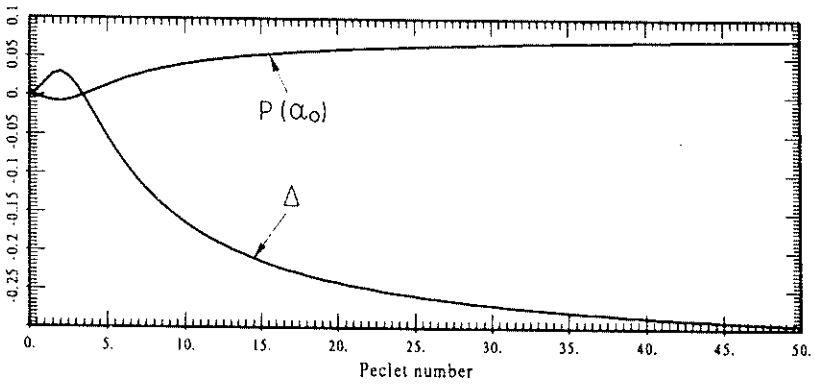

Fig. 4. Discriminant Δ of equation (3.26) and values of $P(\alpha_0)$ for α_0 given by (3.29)

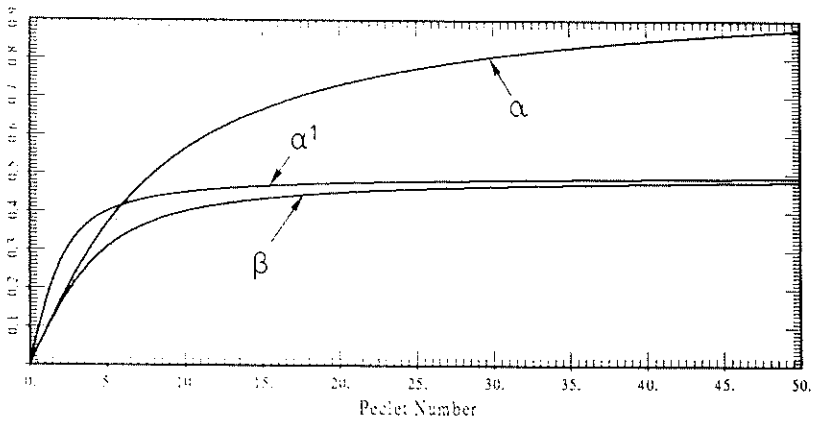

Fig. 5. Upwind functions for quadratic elements

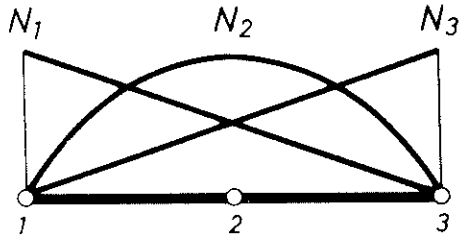

Fig. 6. Hierarchic shape functions for three noded quadratic elements

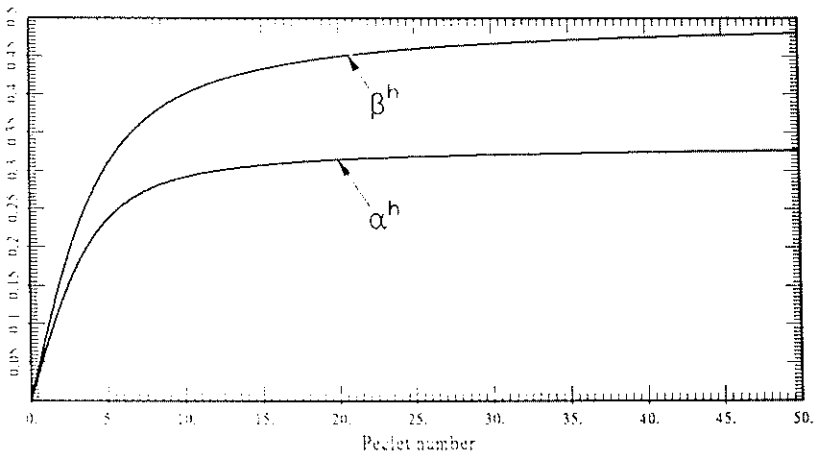

Fig. 7. Upwind functions for hierarchic quadratic elements

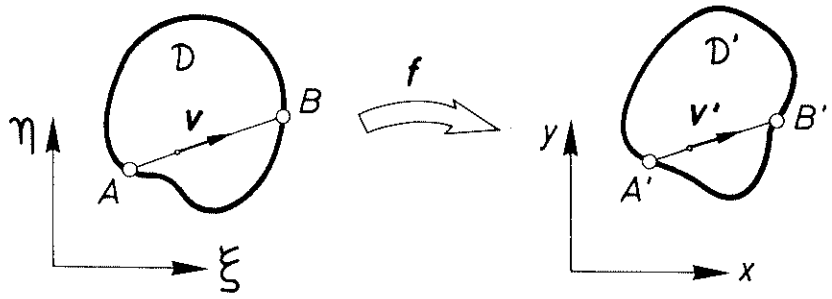

Fig. 8. Transformation of a domain in $\mathbb{R}^2$ by an affine mapping

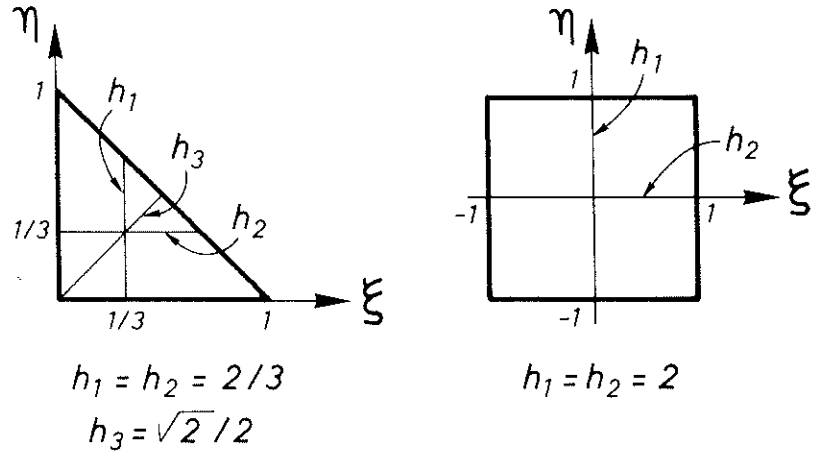

Fig. 9. Parent domains for triangular and quadrilateral elements

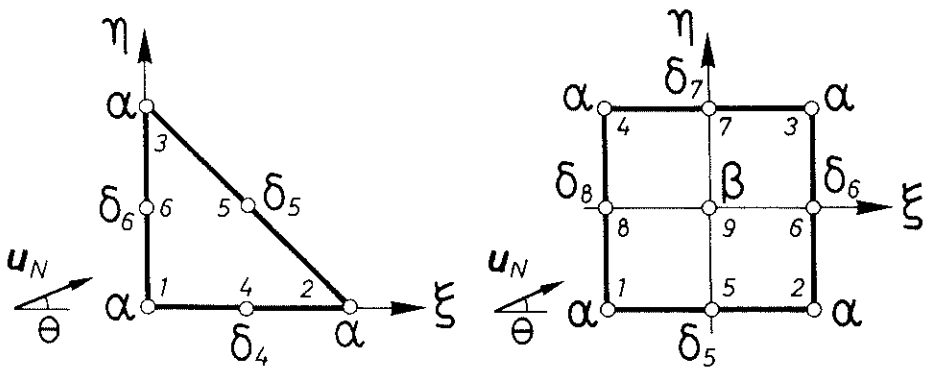

Fig. 10. Assignment of upwind functions for the 6-noded and 9-noded elements

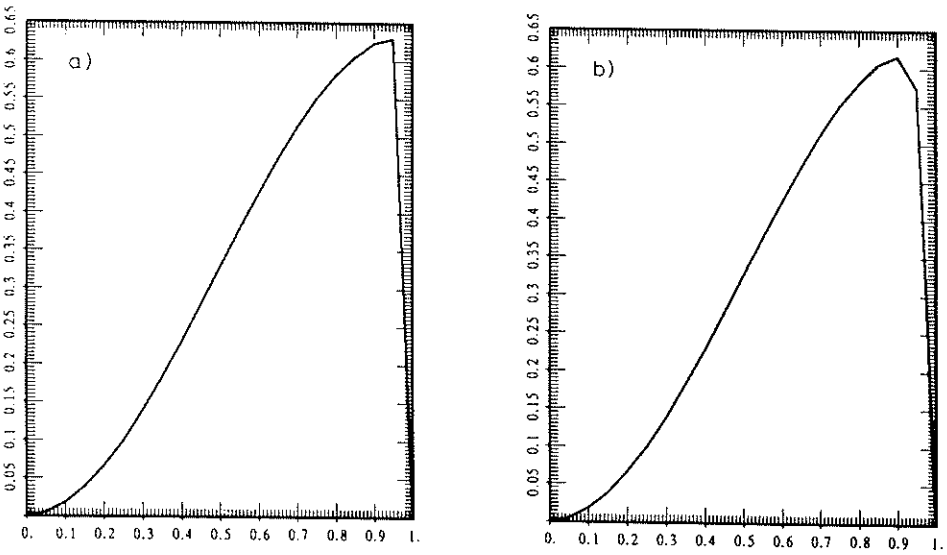

Fig. 11. Solutions of example 1. *a*) Using the upwind functions (3.18) and (3.19). *b*) Using the unique upwind function (3.30)

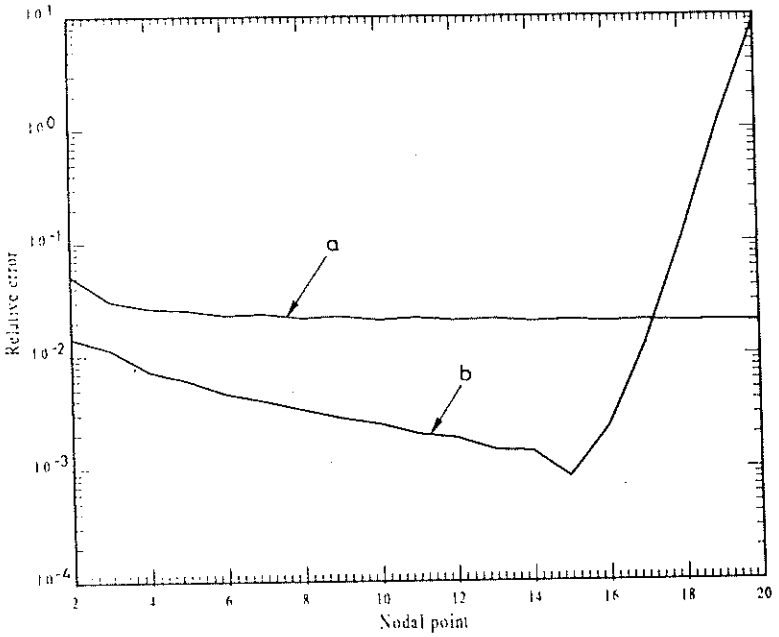

Fig. 12. Relative errors for the solutions a and b of Fig. 11

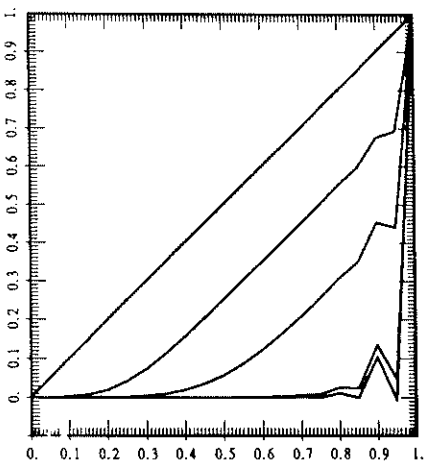

Fig. 13. Galerkin solution of example 2

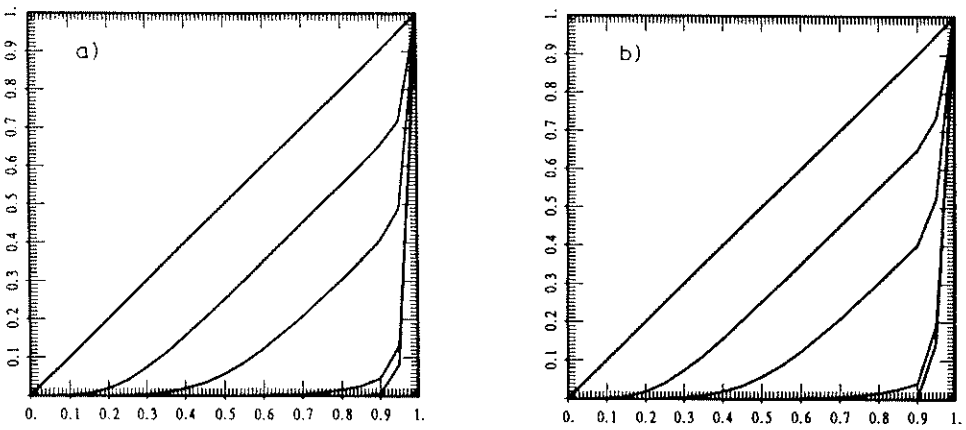

Fig. 14. Solutions of example 2. *a*) Using the upwind functions (3.18) and (3.19). *b*) Using the unique upwind function (3.30)

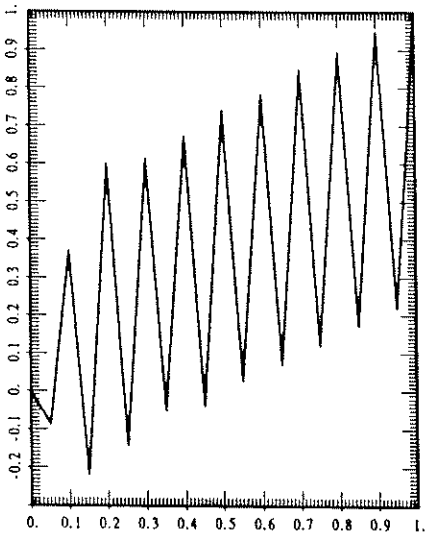

Fig. 15. Galerkin solution of example 3

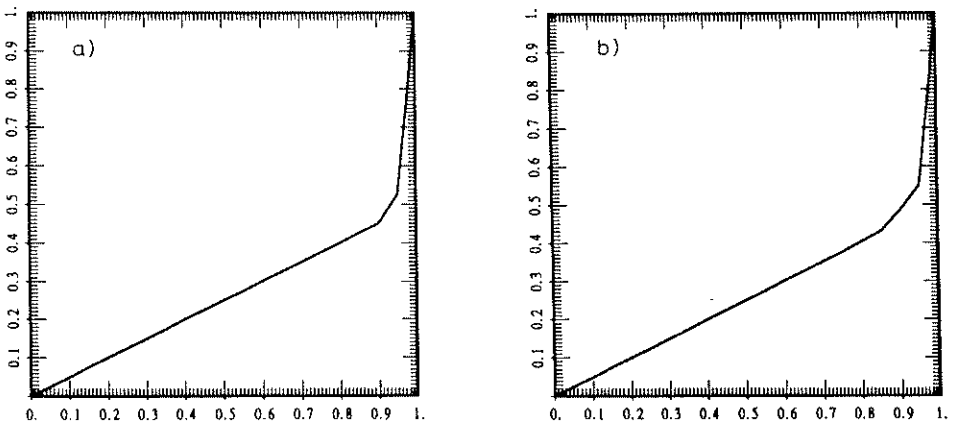

Fig. 16. Solutions of example 3. *a*) Using the upwind functions (3.18) and (3.19). *b*) Using the unique upwind function (3.30)

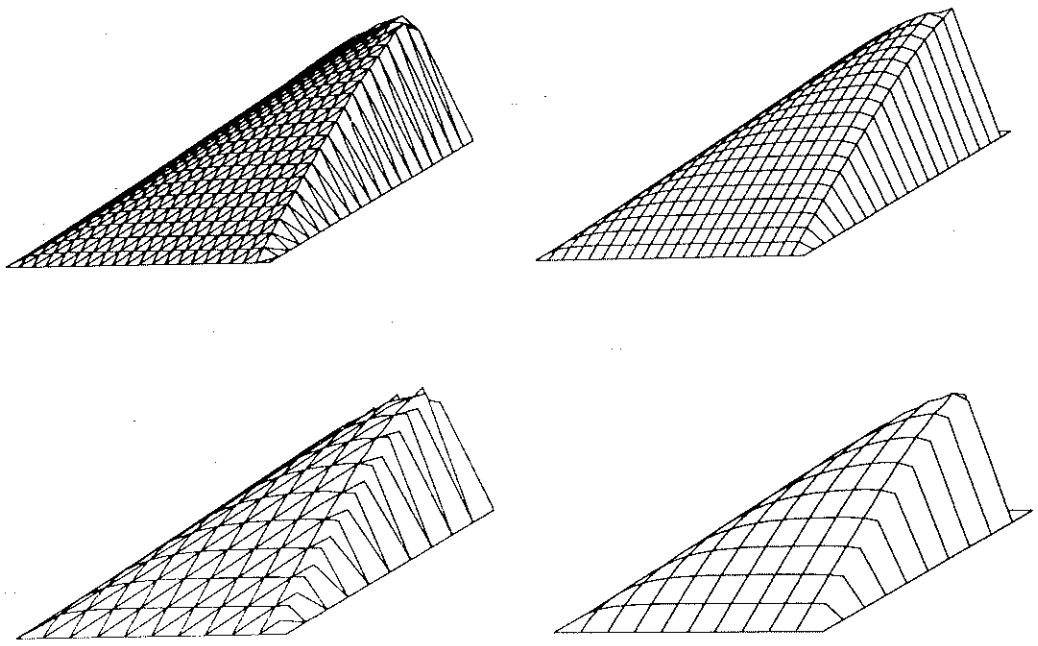

Fig. 17. Results of example 4 using elements of 3, 4, 6 and 9 nodes

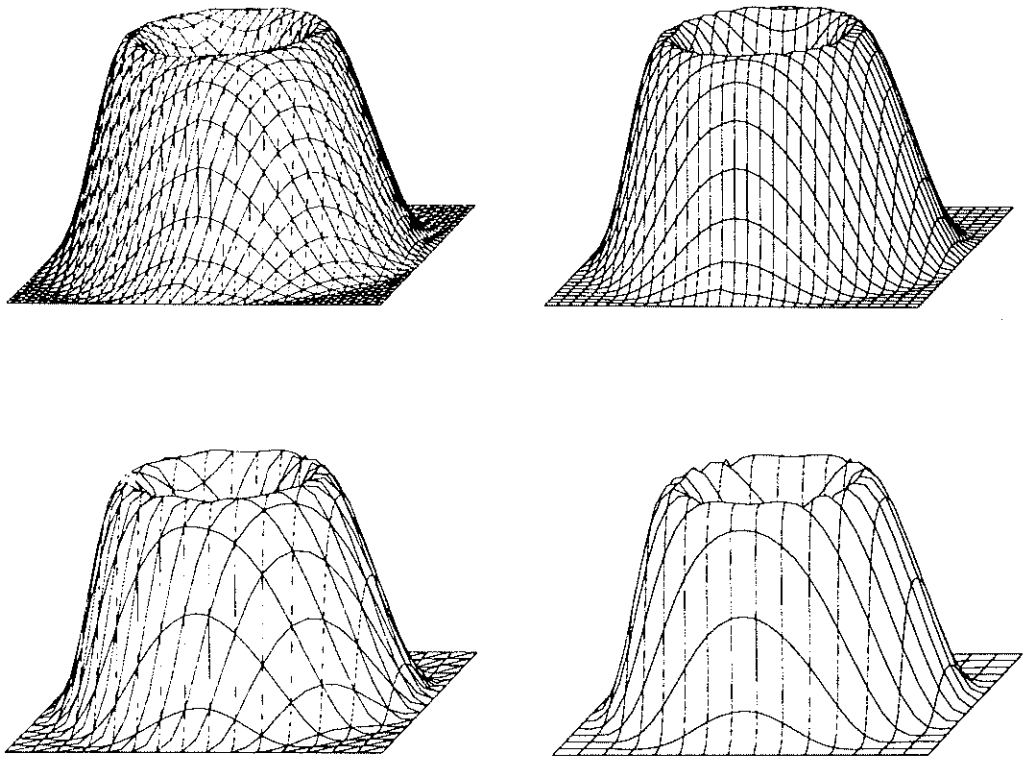

Fig. 18. Results of example 5 using elements of 3, 4, 6 and 9 nodes

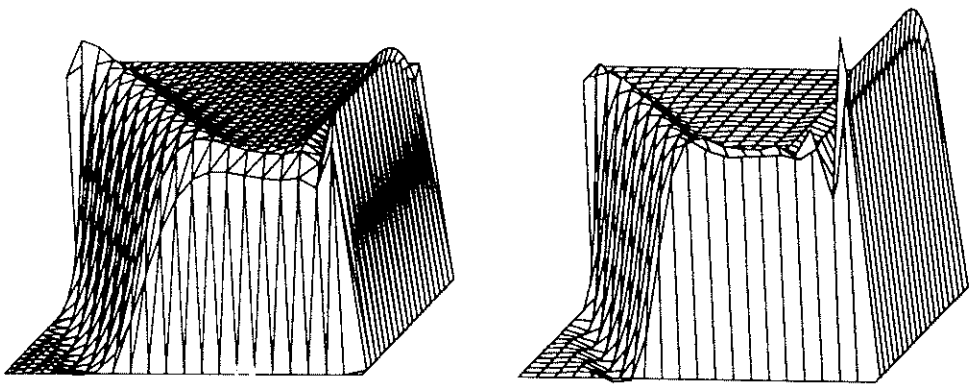

Fig. 19. Results of example 6 using 3-noded linear triangular and 4-noded bilinear quadrilateral elements

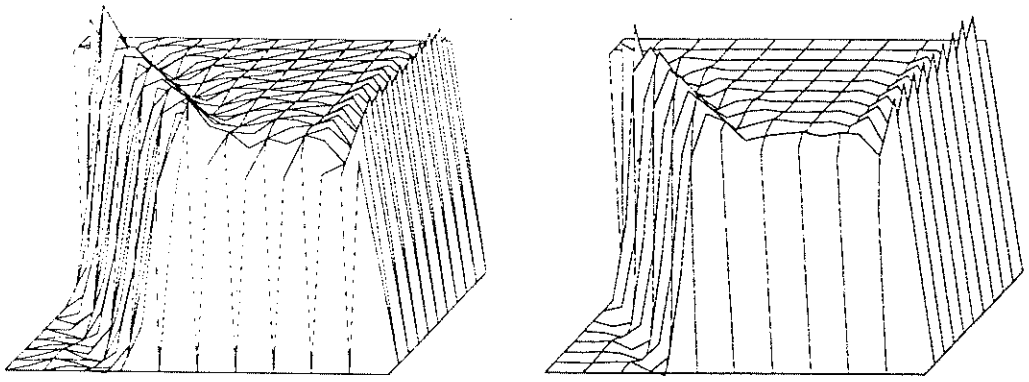

Fig. 20. Results of example 6 using quadratic triangular (6 nodes) and biquadratic quadrilateral (9 nodes) elements with the upwind functions (3.18) and (3.19)

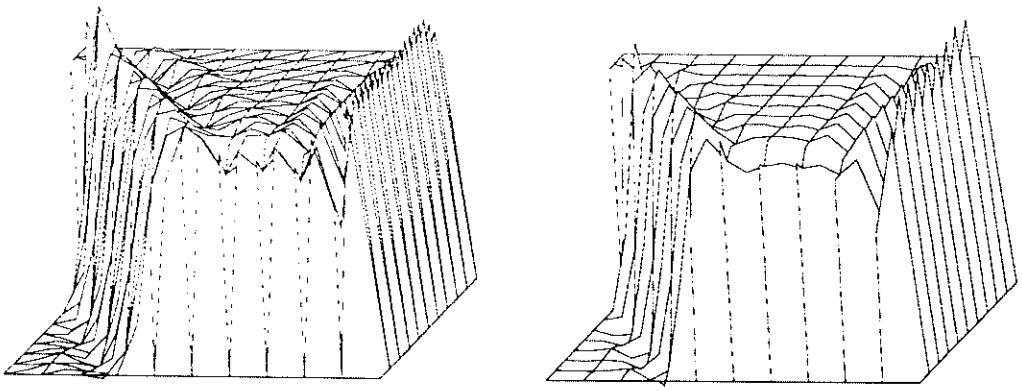

Fig. 21. Results of example 6 using quadratic triangular (6 nodes) and biquadratic quadrilateral (9 nodes) elements with the upwind function (3.30)